



ELSEVIER

EJR

EUROPEAN JOURNAL OF RADIOLOGY

European Journal of Radiology xxx (2008) xxx–xxx

www.elsevier.com/locate/ejrad

Comparison between effective radiation dose of CBCT and MSCT scanners for dentomaxillofacial applications

M. Loubele^{a,b,c,1}, R. Bogaerts^{d,2}, E. Van Dijck^{a,3}, R. Pauwels^{a,4}, S. Vanheusden^{a,5},
P. Suetens^{c,6}, G. Marchal^{e,7}, G. Sanderink^{f,8}, R. Jacobs^{a,b,*}

^a Oral Imaging Centre, School of Dentistry, Oral Pathology and Maxillofacial Surgery, Faculty of Medicine, Katholieke Universiteit Leuven, Kapucijnenvoer 7, 3000 Leuven, Belgium

^b Department of Periodontology, School of Dentistry, Oral Pathology and Maxillofacial Surgery, Katholieke Universiteit Leuven, Kapucijnenvoer 7, 3000 Leuven, Belgium

^c ESAT-PSI, Centre for the Processing of Speech & Images. Department of Electrotechnical Engineering, Group Science, Engineering and Technology, Katholieke Universiteit Leuven, Kasteelpark Arenberg 10 - bus 2440 Belgium

^d Department of Experimental Radiotherapy, University Hospital Gasthuisberg, Katholieke Universiteit Leuven, Herestraat 49 - bus 7003, 3000 Leuven, Belgium

^e Department of Radiology, University Hospital Gasthuisberg, Katholieke Universiteit Leuven, Herestraat 49 - bus 7003, 3000 Leuven, Belgium

^f Oral Radiology Department, ACTA, Louwesweg 5, Amsterdam, The Netherlands

Received 3 January 2008; received in revised form 30 April 2008; accepted 3 June 2008

Abstract

Objectives: To compare the effective dose levels of cone beam computed tomography (CBCT) for maxillofacial applications with those of multi-slice computed tomography (MSCT).

Study design: The effective doses of 3 CBCT scanners were estimated (Accuitomo 3D[®], i-CAT[®], and NewTom 3G[®]) and compared to the dose levels for corresponding image acquisition protocols for 3 MSCT scanners (Somatom VolumeZoom 4[®], Somatom Sensation 16[®] and M×8000 IDT[®]). The effective dose was calculated using thermoluminescent dosimeters (TLDs), placed in a Rando[®] Alderson phantom, and expressed according to the ICRP 103 (2007) guidelines (including a separate tissue weighting factor for the salivary glands, as opposed to former ICRP guidelines).

Results: Effective dose values ranged from 13 to 82 μ Sv for CBCT and from 474 to 1160 μ Sv for MSCT. CBCT dose levels were the lowest for the Accuitomo 3D[®], and highest for the i-CAT[®].

Conclusions: Dose levels for CBCT imaging remained far below those of clinical MSCT protocols, even when a mandibular protocol was applied for the latter, resulting in a smaller field of view compared to various CBCT protocols. Considering this wide dose span, it is of utmost importance to justify the selection of each of the aforementioned techniques, and to optimise the radiation dose while achieving a sufficient image quality. When comparing these results to previous dosimetric studies, a conversion needs to be made using the latest ICRP recommendations.

© 2008 Elsevier Ireland Ltd. All rights reserved.

Keywords: Cone beam CT; Dentomaxillofacial; Effective radiation dose; Multi-slice CT; Jaw

* Corresponding author at: Oral Imaging Centre, Faculty of Medicine, Katholieke Universiteit Leuven, Kapucijnenvoer 7, 3000 Leuven, Belgium.

Tel.: +32 16 33 24 10; fax: +32 16 33 29 51.

E-mail addresses: Miet.Loubele@uzleuven.be (M. Loubele), Ria.Bogaerts@med.kuleuven.be (R. Bogaerts), ruben.pauwels@med.kuleuven.be (R. Pauwels), Paul.Suetens@esat.kuleuven.be (P. Suetens), Guy.Marchal@uzleuven.be (G. Marchal), g.sanderink@acta.nl (G. Sanderink), reinilde.jacobs@med.kuleuven.be (R. Jacobs).

¹ Tel.: +32 16 34 90 44.

² Tel.: +32 16 34 76 37/34 69 13; fax: +32 16 34 76 10.

³ Tel.: +32 16 33 29 51.

⁴ Tel.: +32 16 33 29 51.

⁵ Tel.: +32 16 33 29 51.

⁶ Tel.: +32 16 34 90 26; fax: +32 16 34 90 01.

⁷ Tel.: +32 16 34 37 70/34 37 67; fax: +32 16 34 37 69.

⁸ Tel.: +31 12 05 18 82 60.

1. Introduction

During the last decade, there has been a tendency of using three-dimensional (3D) information to aid in dentomaxillofacial diagnostics and surgery planning [1,2]. Conventional CT protocols are generally associated with relatively high radiation dose levels and even clinical protocols for multi-slice CT (MSCT) still show high doses [3,4]. The introduction of Cone Beam Computed Tomography (CBCT) holds promising potential for oral and craniofacial imaging applications [5–8]. Although the radiation dose of CBCT is generally lower than for MSCT, the use of CBCT may increase the collective radiation dose given for medical purposes disproportional to its frequency of justified utilisation. Therefore, there is a need for reference values for the effective radiation dose for protocols used in CBCT scanners.

Loubele et al. and Guerrero et al. reported radiation dose levels for different MSCTs and CBCTs and related the variation in dose levels to the resulting image quality for various exposure protocols [4,5]. This is an essential relation, although most studies report on either image quality or dose levels. If one would strictly adhere to the ALARA principle, than it is required to try optimising image quality at reasonably low radiation dose levels [9,10]. In a state-of-the-art report on CBCT, Scarfe et al. already discussed the need for optimisation [6]. Few recent studies examined radiation dose levels for CBCT [11,12]. Dose levels varied amongst equipment, exposure protocols and applied methodology. Furthermore, no comparison to spiral CT and MSCT was made. From these data, it is obvious that there is a need for a standardised protocol for effective dose determination for both CBCTs and MSCTs, leading to comparative data which can be generated and reported. This can be accomplished by effective radiation dose estimations using a Rando® Alderson phantom [13,14].

The objective of the present paper is to compare the effective doses of 3 CBCTs for maxillofacial applications with those of corresponding imaging protocols from 3 MSCTs.

2. Materials and methods

2.1. Evaluated CBCT scanners

The following CBCTs were evaluated for radiation dose levels: Accuitomo 3D® (J. Morita Corporation, Kyoto, Japan), NewTom 3G® (Quantitative Radiology, Verona, Italy), and i-CAT® (Imaging Sciences International, Hatfield, Pennsylvania, USA) (Table 1).

The Accuitomo 3D® used in the present study works with an analogue detector. However, it should be noted that the newer Accuitomo 3D FPD® includes a flat panel detector (FPD) with advantages for both image quality and radiation dose levels [15]. The latter also allows a larger field of view while the currently evaluated Accuitomo 3D® had a cylindrical field of view (FOV) of 4 cm dm and 3 cm height. In this study (considering the limited FOV), teeth were divided into three regions to calculate the effective dose: the front, canine-premolar and molar region.

The second CBCT scanner evaluated in this project was the i-CAT®. The i-CAT® was the first CT scanner using a 14 bit FPD. It has several protocols defined by the manufacturer. These protocols were used to compare the effective dose. They are defined by both scan height (6 cm, 8 cm, 13 cm or 22 cm), acquisition time (10 s, 20 s or 40 s) and voxel size (0.1 mm, 0.2 mm, 0.3 mm or 0.4 mm), although the scan time is the most relevant parameter in terms of radiation dose. Voxel size also depends on the reconstruction algorithm (e.g. a 40 s mandible or maxilla scan can be reconstructed in a 0.2 Voxel dataset or a 0.1 Voxel set with a smaller field of view).

The third CBCT scanner, the Newtom 3G®, has a tube current which is determined by the scanner using automatic exposure control, based on a lateral and an anterior topogram of the anatomical area of interest. Three different sizes for the (spherical) FOV could be selected: 6 in., 9 in. and 12 in. which corresponded to a FOV with a diameter of respectively 15.24 cm, 22.86 cm and 30.48 cm. These sizes are defined by the size of

Table 1
Characteristics of the CBCT and MSCT scanners

	3D Accuitomo XII®		i-CAT®		NewTom 3G®	
Gray scale (bit)	12		14		/	
Potential (kV)	60–80		120		110	
Current (mA)	1–10		3–8		<15	
Scan time (s)	18		10, 20, 40		36	
Exposure type	Continuous		Pulsed		Pulsed	
Voxel size (mm)	0.125		0.1–0.4		0.16–0.42	
Object size (mm)	40 × 40, 60 × 60		160 × 130 (220)		100, 150, 200 (diameter)	
Focal Spot (mm)	0.5 × 0.5		0.5 × 0.5		/	
	Somatom VolumeZoom 4®		Somatom Sensation 16®		M×8000 IDT®	
	Head	Mandible	Head	Mandible	Head	Mandible
Potential (kV)	120	120	120	120	120	120
Current (mA)	90	90	90	90	140	140
Scan time (s)	44.12	15.16	29.48	7.87	29.6	7.89
Slice thickness (mm)	0.75	0.75	0.75	0.75	0.75	0.75
Scan Length (mm)	226	72	225	63	225	60
Collimation (mm)	1	1	0.75	0.75	0.75	0.75



Fig. 1. Thermoluminescent dosimeters (left) and the Harshaw Reader 6600® (right).

the imaging detector. Using the 12 in. (30.48 cm) protocol, the whole skull can be acquired. This can be useful in the field of orthognatic surgery, along with other applications. In this study, the 6 in. (15.24 cm) protocol was centred on the maxilla and the mandible in both the axial plane and the z-axis, covering slice 9 till 17 of the phantom. For the 12 in. (30.48 cm) protocol the whole skull was scanned, for the axial positioning it was important that the complete noise was captured. As explained below, the 9 in. (22.86 cm) protocol is used for visualisation of the temporomandibular joint. Although a measurement was performed using this protocol and the resulting effective dose was calculated, it is not included in the table and discarded when comparing the NewTom 3G® with the other CBCT and the MSCT values.

2.2. Evaluated MSCT scanners

A Somatom Volumezoom 4® (Siemens, Erlangen, Germany), Somatom Sensation 16® (Siemens, Erlangen, Germany) and an M×8000 IDT® (Philips Medical Systems, Best, the Netherlands) were used (Table 1). The protocols used are corresponding to those evaluated for CBCT. These protocols were defined by the operator by selecting the tube voltage peak, the product of the tube current and the time, the rotation time, the table feed,

the collimation and the slice width. For comparison with the different CBCT devices (which, as stated above, show a large range in scanned volume), both a full head exposure protocol and a mandibular exposure protocol were used.

2.3. Thermoluminescent dosimeters

Two types of thermoluminescent dosimeters (TLDs) were used: TLD-100 and TLD-100H (Fig. 1). The TLD-100 consist of LiF:Mg,Ti. The TLD-100H, also called supersensitive TLDs, consist of LiF:Mg,Cu,P, which has a lower intrinsic dose detection limit (~1 µSv) than LiF:Mg,Ti (~10 µSv). The latter TLDs were used for dose measurements in organs or tissues which were expected to receive a minimal dose. For each type of TLD 5 non-irradiated TLDs were used to measure the background radiation dose, which was subtracted from the measured dose values. The read-out of the TLDs was performed by a Harshaw Reader 6600® (Fig. 1). Calibration of the TLDs was performed in two steps (Fig. 2). The first step took place every time an experiment was performed. Together with the dosimeters which were used in the experiment, a few internal calibration dosimeters were annealed and irradiated, with a fixed dose delivered by a ⁹⁰Sr source built-in in the reader. The read-out of the calibration dosimeters, preceding the read-out of the field dosimeters,

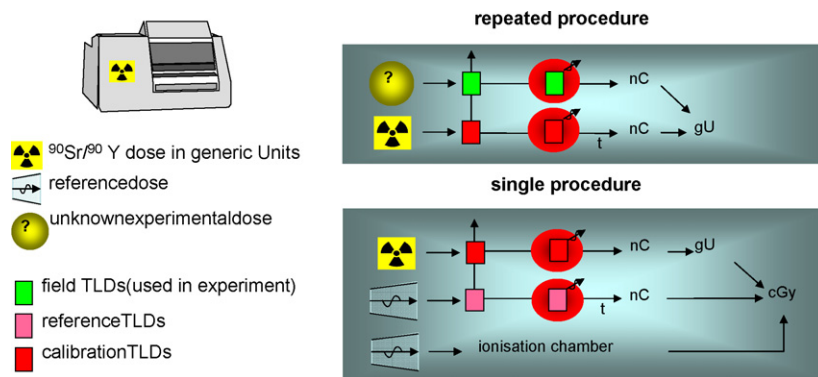


Fig. 2. TLD calibration procedure. In a first, repeated step, a few internal calibration dosimeters are annealed and irradiated with a fixed dose delivered by a ⁹⁰Sr source built-in in the reader. Read-out of these calibration dosimeters yields a conversion factor, which can be applied to the field TLDs. In a second step, the internal source is calibrated using an ionisation chamber as well as reference TLDs.



Fig. 3. Anthropomorphic Rando[®] Alderson phantom, used for measurements on the CBCT devices. Only the 20 slices which were used for TLD placement are shown.

enabled the determination of a conversion factor linking the calibration TLD signal to the fixed internal dose value. The second step is the one-time calibration of the internal source with an ionisation chamber with a calibration factor traceable to a Secondary Standard Dosimetry Laboratory (SSDL; Gent, Belgium). In similar geometric settings and on the same machine as in our experiments, a typical dose was delivered to the ionisation chamber as well as to reference TLDs, which were again linked to a set of internal calibration TLDs. The total uncertainty introduced by the TLD measurement system itself is estimated to be 3–4%.

2.4. Rando[®] Alderson phantom

In the present study, two anthropomorphic male Rando[®] Alderson Phantoms (Rando Alderson Research Laboratories, NY, USA) were used (Fig. 3). Both phantoms represent an average man and consist of a human skeleton embedded in tissue-equivalent material. Considering that pilot experiments have shown that the dose in the lower part of the phantom was negligible in comparison to the dose in the upper part [4], dose level assessment was only performed on the upper 20 slices corresponding to the head and neck region.

2.5. Estimation of the effective radiation dose

Considering the adaptation of the ICRP 1990 recommendations resulting in the ICRP 103 (2007) recommendations, a clear difference and shift in dosimetric reports will become noticeable especially for the head and neck region, as salivary glands have now and for the first time received a distinct weighting factor, expressing their radiosensitivity (Table 2) [3,16–19]. The tissue weighting factors represent the contribution of the risk of stochastic radiation effects for that organ or tissue to the overall risk [13].

The effective dose was selected for assessment as it reflects a good clinical and standardised measurement for the biological effects of irradiation, although previous studies have shown

Table 2
Tissue weighting factors in ICRP recommendation documents

Organ	ICRP 60	ICRP 103
Gonads	0.2	0.08
Red bone marrow	0.12	0.12
Colon	0.12	0.12
Lung	0.12	0.12
Stomach	0.12	0.12
Bladder	0.05	0.04
Breast	0.05	0.12
Liver	0.05	0.04
Oesophagus	0.05	0.04
Thyroid	0.05	0.04
Skin	0.01	0.01
Bone surface	0.01	0.01
Brain	0	0.01
Salivary glands	0	0.01
Remainder ^a	0.05	0.12

^a Remainder tissues are: adipose tissue, adrenals, connective tissue, extrathoracic airways, gall bladder, heart wall, lymphatic nodes, muscle, pancreas, prostate, si wall, spleen, thymus, and uterus/cervix.

some limitations on the use of the effective dose. A study by Ludlow et al. shows a good overall reproducibility (2.5% variation between repeated identical examinations), although some specific TLD locations showed a large variation [11]. It is clear that effective dose estimations are dependent on many factors which are not standardised, such as the phantom itself (e.g. real bone versus bone-equivalent material), the number of TLDs and their placement. Furthermore, since effective dose is supposedly measured on an average person (male, female or child), it serves as an estimation which should not be readily applied to a patient. As mentioned by Martin, there is a large uncertainty ($\pm 40\%$) in the effective dose for a reference patient [20]. The definition of patient-dependent conversion factors for effective dose should definitely be further investigated.

The measurements were performed by inserting TLDs at different positions within different slices of the organs or tissues of interest. The phantom was irradiated 10 times to enlarge the dose substantially above the background dose values. In order to calculate the equivalent doses H_T for all organs or tissues T, the following formula was used:

$$H_T = w_R \sum f_i D_{Ti} \quad (1)$$

with w_R the radiation weighting factor, being 1 for X-rays, D_{Ti} the average absorbed dose of organ T in slice i , and f_i the fraction of organ T in slice i . The equivalent organ dose has to be multiplied by the tissue weighting factor w_T to obtain the contribution E_T of the organ to the effective dose.

$$E_T = w_T \cdot H_T \quad (2)$$

Summing all contributions E_T thus provides the effective dose E .

3. Results

Table 3A shows the effective dose for the different acquired regions, along with the relative organ distribution of the dose of

Table 3A
Effective organ doses and total effective dose (μSv) for the different protocols of the Accuitomo 3D[®] and the i-CAT[®]

WT	Accuitomo 3D [®]						i-CAT [®]											
	Upper jaw			Lower jaw			8 cm, 40 s			Extended field of view, 2 x 20 s			Mand, 20 s	Mand, 40 s	Max, 20 s	Max, 40 s		
	Front	Premolar and canine	Molar	Front	Premolar and canine	Molar	Front	Premolar and canine	Molar	Front	Premolar and canine	Molar	Front	Premolar and canine	Molar	Front	Premolar and canine	Molar
Gonads	0.08	0	0	0	0	0	0	0	0	0	0	0	0	0	0	0	0	0
Red bone marrow	0.12	23	37	8	12	19	11	26	0	17	33	0	0	22	46	0	0	0
Colon	0.12	0	0	0	0	0	0	0	0	0	0	0	0	0	0	0	0	0
Lung	0.12	0	0	0	0	0	0	0	0	0	0	0	0	0	0	0	0	0
Stomach	0.12	0	0	0	0	0	0	0	0	0	0	0	0	0	0	0	0	0
Bladder	0.04	0	0	0	0	0	0	0	0	0	0	0	0	0	0	0	0	0
Breast	0.12	0	0	0	0	0	0	0	0	0	0	0	0	0	0	0	0	0
Liver	0.04	0	0	0	0	0	0	0	0	0	0	0	0	0	0	0	0	0
Oesophagus	0.04	0	0	0	0	0	0	0	0	0	0	0	0	0	0	0	0	0
Thyroid	0.04	1	1	2	6	2	8	12	5	9	9	2	4	10	7	2	2	4
Skin	0.01	1	0	0	0	0	1	2	0	0	2	0	2	10	2	0	0	0
Bone surface	0.01	2	3	1	1	2	1	2	1	1	3	1	3	2	4	2	2	4
Salivary glands	0.01	2	2	3	3	6	9	20	10	15	15	3	5	5	11	3	3	8
Brain	0.01	1	1	0	0	0	8	20	0	0	3	0	3	3	8	0	0	0
Remainder	0.12	0	0	0	0	0	0	0	0	0	0	0	0	0	0	0	0	0
Total	29	44	44	13	22	29	37	82	34	64	64	34	45	45	77	0	0	0

s = seconds, mand = mandible, max = maxilla.

the Accuitomo 3D[®] and i-CAT[®]. Table 3B shows the effective dose and organ distribution for two additional protocols of the i-CAT[®] and for the NewTom 3G[®].

For the Accuitomo 3D[®], the highest effective dose is found for the premolar and canine upper jaw region (44 μSv) and the lowest effective dose for the front lower jaw region (13 μSv). The red bone marrow absorbs the highest dose followed by the salivary glands, bone surface and thyroid. The skin has the lowest contribution to the effective dose. Many tissues with a distinct weighting factor, such as liver, stomach and bladder, do not show any dose since pilot studies have indicated that TLD placement in these organs did not yield a significant dose considering the more distant radiation beam. These organs are listed in the table in order to include all weighting factors.

For the i-CAT[®], the 'extended field of view 40 s' option showed the highest dose and the 'mandible 20 s' protocol the lowest, with the effective dose ranging between 34 and 82 μSv . Also, with this device the consistency between upper and lower jaw was less clear, with dose levels recorded for the mandible often being lower than those for the maxilla. Considering the individual organs, in general, red bone marrow, thyroid and salivary glands received a higher dose while skin and brain received a lower dose.

For the NewTom 3G[®], the 9 in. (22.86 cm) protocol was not included in the table because of its substantially higher effective dose (191 μSv , with a huge organ dose for the thyroid gland), compared to the other two protocols. It was positioned on the condyle, leading to higher automatic exposure settings (40 mAs compared to 9 mAs for the other protocols) because of the dense bone structures in that area. Therefore, this measurement would fall into a separate category of TMJ acquisitions, which are performed using higher current settings. When discarding the 9 in. protocol, the 6 in. protocol results in the highest effective radiation dose with 57 μSv . The 12 in. protocol results in the least dose with 30 μSv . The contribution to the effective dose is highest for the salivary glands, followed by the thyroid gland and the bone surface.

Fig. 4 shows an estimation of the required dose for a patient scan using two different clinical indications. When requiring a larger FOV than that which the Accuitomo 3D[®] can acquire in a single scan, the cumulative dose from the latter could surpass that of an i-CAT[®] or a NewTom 3G[®] scan. However, as mentioned before, there is a large uncertainty when applying effective doses to reference patients [20].

Table 3C shows the effective dose for the MSCT devices. The Somatom VolumeZoom 4[®] showed an effective dose of 1110 μSv for the full head exposure protocol. The thyroid has the largest contribution to the effective dose, followed by the red bone marrow and the salivary glands. When just the mandible was scanned, effective dose is 494 μSv . The highest organ dose was found for the salivary glands followed by the thyroid and the red bone marrow.

For the Somatom Sensation 16[®], the highest effective dose for the full head exposure protocol was 994 μSv . The highest contributions came from the thyroid gland, red bone marrow, and salivary glands. For the mandibular protocol, effective dose was 474 μSv . The salivary glands had the highest contribution

Table 3B
Effective organ doses and total effective dose (μSv) for the different protocols of the NewTom 3G[®] and the i-CAT[®]

	W_T	NewTom 3G [®]		I-CAT [®]	
		6"	12"	13 cm 10 s	13 cm 40 s
kVp		110	110	120	120
mAs		9.1	9.0	10.6	39.5
Gonads	0.08	0	0	0	0
Red bone marrow	0.12	16	1	0	0
Colon	0.12	0	0	0	0
Lung	0.12	0	0	0	0
Stomach	0.12	0	0	0	0
Bladder	0.04	0	0	0	0
Breast	0.12	0	0	0	0
Liver	0.04	0	0	0	0
Oesophagus	0.04	0	0	0	0
Thyroid	0.04	8	9	10	20
Skin	0.01	0	0	0	0
Bone surface	0.01	8	6	27	20
Salivary glands	0.01	22	13	11	37
Brain	0.01	3	1	0	0
Remainder	0.12	0	0	0	0
Total	1	57	30	48	77

to the effective dose, followed by the red bone marrow and the thyroid gland.

The Philips M \times 8000 IDT also showed a much higher dose for the full head protocol (1160 μSv) compared to the mandibular exposure protocol (541 μSv). Organ distributions were also similar to the other 2 MSCT devices, with high contributions

coming from the salivary glands, thyroid and red bone marrow.

Table 4 shows effective doses for all devices and protocols used in this study, as well as the recalculated effective dose (using the ICRP 103 recommendations) of two previously published studies, using panoramic radiography and tomography. Protocols for CBCT and MSCT were divided into those with a small and a large FOV, although these two groups still show a large variation in acquired volume between the CBCT devices. The radiation dose of CBCT scanners is between 2 times (for the Accuitomo 3D[®]) and about 15 times (for the i-CAT[®] extended FOV) higher as that of a traditional dental radiography unit. When converting the results by Gijbels et al. to the ICRP 103 tissue weighting factors, effective dose for the 5 panoramic scanners ranges between 3 and 8 μSv [21]. Furthermore, CBCT dose levels appear to be in the same range as those of traditional tomography. Converting the study by Dula et al., effective dose for tomography ranged between 28 and 88 μSv [22].

4. Discussion

As demonstrated before, the introduction of Cone Beam Computed Tomography (CBCT) holds promising potential for oral and craniofacial imaging applications [5–8]. The radiation dose of different CBCT scanners was compared with different MSCT scanners. The radiation dose was evaluated by effective dose measurements on Rando[®] Alderson phantoms.

A huge difference in effective dose between CBCT and MSCT can be observed, with effective dose ratio's up to 90. However, especially for the Accuitomo 3D[®], the huge difference in FOV (especially compared to the MSCT full head protocols) renders it hard to make a fair comparison based on effective dose alone. Still, there is a noticeable gap between the MSCT and CBCT dose ranges. A study by Tsiklakis et al. on CBCT dose versus conventional CT dose mentions a 8- to 10-fold reduction in dose for CBCT compared to conventional CT [12]. When

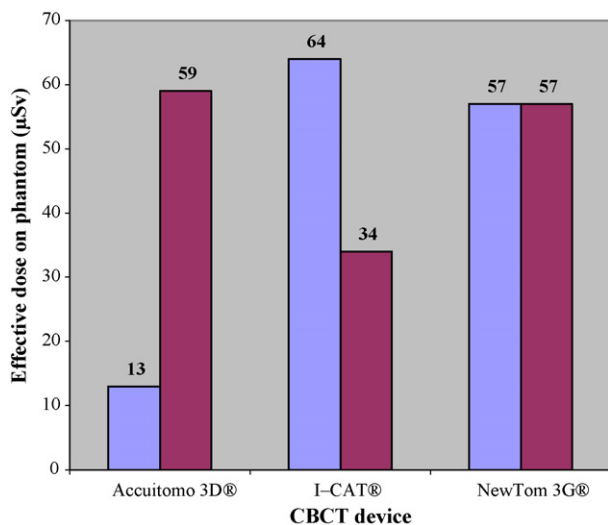


Fig. 4. Estimation of the effective dose (in μSv) for two clinical indications. In blue: pre- or post-operative scan for rehabilitation of an edentulous lower jaw by means of oral implants. In red: scan for extraction of impacted teeth in vicinity of mandibular canal. Note: the effective dose of the Accuitomo 3D[®] was doubled for the second indication, because of the need for two scans in the left and right molar region. For the NewTom 3G[®], effective dose will vary for the two different indications in reality, because the field of view will be centered slightly different, leading to a change in exposure settings and dose uptake. The protocols chosen for the different devices were the ones that suited best for this application (Accuitomo 3D[®]: 80 kV 4 mA front region and 80 kV 4 mA premolar region. I-CAT: Mand 40 s 0.2 Voxel and Mand 20 s 0.3 Voxel. NewTom 3G[®]: 6" (15.24 cm) field of view).

Table 3C

Effective organ doses and total effective dose (μSv) for the different protocols of the MSCT scanners

	W_T	Somatom VolumeZoom 4 [®]		Somatom Sensation 16 [®]		Philips M \times 8000 IDT [®]	
		Mandible	Head	Mandible	Head	Mandible	Head
Gonads	0.08	0	0	0	0	0	0
Red bone marrow	0.12	92	317	78	328	31	343
Colon	0.12	0	0	1	0	1	0
Lung	0.12	34	68	35	53	26	64
Stomach	0.12	0.0	0.0	4	0.0	4	0.0
Bladder	0.04	0	0	0	0	0	0
Breast	0.12	0	0	0	0	0	0
Liver	0.04	1	1	2	0.9	1.9	1
Oesophagus	0.04	17	28	19	25	2	30
Thyroid	0.04	169	357	213	270	325	361
Skin	0.01	5	12	4	11	5	11
Bone surface	0.01	7	25	6	26	5	27
Salivary glands	0.01	150	154	99	144	113	165
Brain	0.01	13	139	8	131	13	149
Remainder	0.12	7	11	7	7	14	9
Total	1	494	1110	474	995	541	1160

comparing similar FOVs between MSCT and CBCT datasets (e.g. the i-CAT[®] extended FOV with the MSCT full head protocols, the i-CAT[®] mandible protocol with the MSCT mandible protocols, the NewTom[®] 6'' FOV with the MSCT mandible protocols), a dose reduction of more than 10-fold can be observed. When a low dose protocol for MSCT would be applied, there is a significant reduction in effective dose, leading to more comparable values. However, one should bear in mind that these protocols are not daily used for routine clinical applications, mainly due to the post-processing needed to improve image quality. Regardless of this, the use of MSCT for dentomaxillofacial applications often leads to a much higher image quality than needed for diagnostic purposes. In many cases, the additional radiation dose compared to CBCT is not justified.

Focusing on the Accuitomo 3D[®], a certain consistency can be observed in the results. The upper jaw receives a higher dose than the lower jaw, with as only exception the molar region. An explanation for this phenomenon could be that the lower jaw consists of a thicker bone segment than the upper jaw, which causes a larger attenuation of the X-rays. The exception of the molar region could be a consequence of the presence of the zygoma, a thick bone concentrated in this region. In other applications, we notice the same trend. Bou Serhal et al. carried out a study on spiral CT and conventional spiral tomography [23,24]. Their results were separated in upper and lower jaw dose at one hand and radiation dose at the same site or the opposite site of the source on the other hand. Their straightforward conclusion is that the region situated in the primary beam of the X-ray source gets the highest dose. For CT examinations, both of the parotid glands are situated within the primary beam and therefore receive the highest dose. During CT of the lower jaw, the submandibular glands receive the highest dose.

For the separate contributions of the organs to the effective dose from the Accuitomo 3D[®], the upper jaw scans result in higher organ doses than those of the lower jaw. Two exceptions can be found. First, the salivary glands receive the highest dose

in the lower molar region. Because of the high doses to these glands, the lower molar region contributes almost as much to the effective dose as the upper molar region, while normally the upper jaw contributes almost twice as much as the lower jaw. The second exception is observed for the thyroid measurements. This organ receives the highest dose when imaging the premolar and canine region of the lower jaw, which is due to the position of the thyroid nearby this region.

Comparing the effective dose for all three CBCT scanners (again discarding the NewTom 3G[®] value from the 9 in. protocol), the highest radiation dose is measured for the two largest protocols (in terms of field of view and resolution) of the i-CAT[®]. The lowest doses are for 5 out of 6 protocols of the Accuitomo 3D[®]. These relatively low doses of the Accuitomo 3D[®] can be partly explained by the small FOV in comparison with the FOVs for the i-CAT[®] and the NewTom 3G[®]. This extra volume represents an extra radiation dose, which does not always coincide with a diagnostic benefit. Depending on the indication, the Accuitomo[®] may be advised for localised problems, gaining enough information at a low dose. However, for particular indications, a larger region needs to be scanned (spanning the entire jaw or part of it) which would require multiple scans with the Accuitomo[®], resulting in a summation of the radiation doses reported in this study, as demonstrated in Fig. 4.

When contrasting the present results to former studies, one should be aware that previous dose level calculations in the jaw bone region may have over- or underestimated the effective radiation dose. Salivary gland tissue radiation was often not included in effective dose calculations (Table 2). However, previous studies have pointed out that a high dose can be received by the salivary glands in dental radiology [3,17–19]. Therefore, it was often considered as a remainder tissue when performing dental dosimetry, receiving a weighting factor up to 0.025 because of its high radiation weighted dose [11,12,19,21]. Also, in the new ICRP 103 recommendations the thyroid has received a slightly lower weighting factor, resulting in a lower contribution for this

Table 4

Comparison between effective dose of CBCT and MSCT devices, and previous studies using panoramic radiography and tomography (converted using the ICRP 103 tissue weighting factors)

Device and acquisition mode	Effective dose (ICRP 103)
CBCT, large volume	
NewTom 3G, 6" FOV	57
NewTom 3G, 12" FOV	30
I-CAT, 13 cm 10 s	48
I-CAT, 13 cm 40 s	77
I-CAT, extended field of view, 2 × 20 s	82
MSCT, full head	
Somatom VolumeZoom 4	1110
Somatom Sensation 16	995
Philips M×8000 IDT	1160
CBCT, small volume	
Accuitomo 3D, upper jaw, front region	29
Accuitomo 3D, upper jaw, premolar and canine region	44
Accuitomo 3D, upper jaw, molar region	29
Accuitomo 3D, lower jaw, front region	13
Accuitomo 3D, lower jaw, premolar and canine region	22
Accuitomo 3D, lower jaw, molar region	29
I-CAT, 8 cm, 40 s	37
I-CAT, Mand, 20 s	34
I-CAT, Mand, 40 s	64
I-CAT, Max, 20 s	45
I-CAT, Max, 40 s	77
MSCT, mandible	
Somatom VolumeZoom 4	494
Somatom Sensation 16	474
Philips M×8000 IDT	541
Panoramic radiography, Gijbels et al. [21]	
Cranex Tome	5
Cranex Excel	7
Veraviewepocs 5D	3
EC Proline	8
Orthoralix 9200 DDE	3
Tomography, Dula et al. [22]	
Cranex Tome, region 16	47
Scanora D, region 16	83
Cranex Tome, region 46	28
Scanora D, region 46	88

organ which seems to overcompensate for the salivary glands, finally resulting in a slight reduction or status quo in total effective dose [16], except for those studies in which the salivary glands were included as remainder tissue; in these cases, a conversion to ICRP 103 yields a much lower effective dose. For a correct interpretation of the results, dose levels should be compared using the same standard, in this case the latest ICRP 103 guidelines.

In conclusion, dose levels for CBCT imaging remained far below those of clinical MSCT protocols, and showed a large inter- and intra-device variation due to differences in exposure settings, field of view and spatial resolution. All relevant factors should be considered when justifying the selection of these techniques. Radiation dose needs to be kept as low as possible at all times, optimising its balance with image quality.

References

- [1] van Steenberghe D, Naert I, Anderson M, Brajnovic I, Van Cleynenbreugel J, Suetens P. A custom template and definitive prosthesis allowing immediate implant loading in the maxilla: a clinical report. *Int J Oral Maxillofac Implants* 2002;17:663–7.
- [2] Gahleitner A, Watzek G, Imhof H. Dental CT: imaging technique, anatomy, and pathologic conditions of the jaws. *Eur Radiol* 2003;13:366–410.
- [3] Cohnen M, Kemper J, Mobes O, Pawelzik J, Modder U. Radiation dose in dental radiology. *Eur Radiol* 2002;12:634–7.
- [4] Loubele M, Jacobs R, Maes F, et al. Radiation dose vs. image quality for low-dose CT protocols of the head for maxillofacial surgery and oral implant planning. *Radiat Prot Dosimetry* 2006;117:211–6.
- [5] Guerrero ME, Jacobs R, Loubele M, Schutyser F, Suetens P, van Steenberghe D. State-of-the-art on cone beam CT imaging for preoperative planning of implant placement. *Clin Oral Invest* 2006;10:1–7.
- [6] Scarfe WC, Farman AG, Sukovic P. Clinical applications of cone-beam computed tomography in dental practice. *J Can Dent Assoc* 2006;72:75–85.
- [7] Dreiseidler T, Ritter L, Keeve E, Mischkowski RA, Neugebauer J, Zöllner JE. Usability of the cone beam technique for three-dimensional pre-surgical dental implant treatment planning. *Int J Cars* 2006;1:389–402.
- [8] Lascala CA, Panella J, Marques MM. Analysis of the accuracy of linear measurements obtained by cone beam computed tomography (CBCT-NewTom). *Dentomaxillofac Radiol* 2004;33(5):291–4.
- [9] Martin CJ, Sutton DG, Sharp PF. Balancing patient dose and image quality. *Appl Radiat Isot* 1999;50(1):1–19.
- [10] Farman AG. ALARA still applies. *Oral Surg Oral Med Oral Pathol Oral Radiol Endod* 2005;100:395–7.
- [11] Ludlow JB, Davies-Ludlow LE, Brooks SL, Howerton WB. Dosimetry of 3 CBCT devices for oral and maxillofacial radiology: CB Mercuray NewTom 3G and i-CAT. *Dentomaxillofac Radiol* 2006;35:219–26.
- [12] Tsiklakis K, Donta C, Gavala S, Karayianni K, Kamenopoulou V, Hourdakis CJ. Dose reduction in maxillofacial imaging using low dose Cone Beam CT. *Eur J Radiol* 2005;56(3):413–7 [Epub 2005 June 22].
- [13] Golikov VY, Nikitin VV. Estimation of the mean organ doses and the effective dose equivalent from Rando phantom measurements. *Health Phys* 1989;56:111–5.
- [14] Huda W, Sandison GA. Estimation of mean organ doses in diagnostic radiology from Rando phantom measurements. *Health Phys* 1984;47:463–7.
- [15] Spahn M. Flat detectors and their clinical applications. *Eur Radiol* 2005;15:1934–47.
- [16] ICRP Publication 103. Radiation protection. Recommendations of the International Commission on Radiological Protection. Pergamon Press; 2007.
- [17] Christiansen EL, Moore RJ, Thompson JR, Hasso AN, Hinshaw Jr DB. Radiation dose in radiography CT and arthrography of the temporomandibular joint. *AJR Am J Roengenol* 1987;148:107–9.
- [18] Ludlow JB, Davies-Ludlow LE, Brooks SL. Dosimetry of two extraoral direct digital imaging devices: Newtom cone beam CT and Orthophos Plus PS panoramic unit. *Dentomaxillofac Radiol* 2003;32:229–34.
- [19] Lecomber AR, Downes SL, Mokhtari M, Faulkner K. Optimisation of patient doses in programmable dental panoramic radiography. *Dentomaxillofac Radiol* 2000;29:107–12.
- [20] Martin CJ. Effective dose: how should it be applied to medical exposures? *Br J Radiol* 2007;80(956):639–47 [Epub 2007 July 23].
- [21] Gijbels F, Jacobs R, Bogaerts R, Debaveye D, Verlinden S, Sanderink G. Dosimetry of digital panoramic imaging Part I: patient exposure. *Dentomaxillofac Radiol* 2005;34(3):145–9.
- [22] Dula K, Mini R, van der Stelt PF, Sanderink GC, Schneeberger P, Buser D. Comparative dose measurements by spiral tomography for preimplant diagnosis: the Scanora machine versus the Cranex Tome radiography unit. *Oral Surg Oral Med Oral Pathol Oral Radiol Endod* 2001;91(6):735–42.
- [23] Bou Serhal C, van Steenberghe D, Bosmans H, Sanderink G, Quirynen M, Jacobs R. Organ radiation dose assessment for conventional spiral tomography: a human cadaver study. *Clin Oral Impl Res* 2001;12:85–90.
- [24] Bou Serhal C, Jacobs R, Gijbels F, et al. Absorbed doses from spiral CT and conventional spiral tomography: a phantom vs cadaver study. *Clin Oral Impl Res* 2001;12:473–8.